# DEVELOPMENT AND APPLICATION OF MODELS FOR THE STABILITY ANALYSIS OF AUSTRALIA'S OFFSHORE PIPELINES

**M.J. Cassidy and Y. Tian**
*Centre for Offshore Foundation Systems, University of Western Australia*

## ABSTRACT

Offshore subsea pipelines are used to export oil and gas from the field to platform and then from the platform to the mainland. As they are the sole conduit for the hydrocarbons their stability and integrity are of critical economic and environmental importance. With more than 80 per cent of Australia's gas resources in deep, remote, offshore areas, the ability to realise their full potential relies on the development of safe and economically viable solutions to transport them. Pipelines offshore Australia must maintain structural integrity and continuous supply of products across hundreds of kilometres of seabed. This paper discusses one aspect of this challenge. It concentrates on how to design for stability of untrenched pipelines under storm conditions. Force balance methods commonly applied are first described before the benefits of using a dynamic time domain approach are shown by way of example. Novel macroelement plasticity models that describe the force-displacement behaviour of a vertically and laterally loaded pipe in Australian soils are outlined. Their application is shown in the design example.

## 1 INTRODUCTION

Building a pipeline system to link an offshore oil and gas field to the mainland represents a huge capital investment. For example, in Australia the construction of the 42 inch 135 km pipeline for the Trunkline System Expansion Project (TSEP) on the North West Shelf in 2003/04 cost approximately A$800 million. Today, the cost per kilometre of current pipeline projects, including the Gorgon (water depth:1350 m length: 65 and 140 km), Scarborough (depth: 900 m length: 280 km), Pluto (depth: 830 m length: 180 km) and Browse (depth: 600m length: 5, 24 and 400 km) is estimated to exceed $4.5 million per km. With over 2000 km of pipelines under design in Australia, capital expenditure is expected to exceed $10 billion. Table 1 provides a summary of notable pipelines built or under consideration offshore Western Australia.

In Australia pipelines are laid directly on the seabed, and as shown in Table 1, are mainly large diameter, but light gas pipes. One of the most fundamental engineering tasks is to ensure their on-bottom stability under the action of hydrodynamic loads from waves and currents. On the North West Shelf of Australia pipeline stabilisation is a major cost driver. Shallow water, complex calcareous soil conditions and severe environmental loading from summer tropical cyclones form a challenging environment. Overly conservative 'primary' designs that simply increase the pipe weight with concrete cover quickly become uneconomical. Even the use of 'secondary' stabilisation, such as anchors, flexible concrete mattresses or rock dump, can represent as much as 30% of the total pipeline capital expenditure (Brown *et al.,* 2002. Examples of anchor systems used on the North West Shelf of Australia are shown in Figure 1. These engineered anchors, in this case of length 5.5 m, width 3.3 m, height 2.3 m and weight 31 tonnes, are costly to install. There is significant incentive for development of more accurate analysis and design methods.

This paper discusses methods to predict the stability of untrenched pipelines in large offshore storms. The three main approaches used by industry are first discussed. These consist of a simplistic force-balance method, where no pipe movement is assumed, design charts available in industry guidelines and a dynamic time domain approach where the prediction of the movement of the entire pipeline is evaluated. An aim of the paper is to review the development of state-of-the-art models that allow more accurate and efficient calculations in this latter time domain analysis. These macroelement plasticity models are finding increasing use as a tool to describe the vertical and horizontal behaviour of a pipe segment more accurately. An additional advantage is that they can be incorporated directly into the structural analysis programs used by engineers on a daily basis. Models for drained behaviour in calcareous sands and silts and for undrained behaviour in clays are described. The final aim of the paper is to present a simple design scenario and to show the benefit of the new models and the time domain approach.

There are many other geotechnical problems related to the design of offshore pipelines. These include, amongst others, soil characterisation, self-burial, trenching, pipe-laying, ploughing, pipeline buckling and walking, and the impact of geohazards such as submarine landslides. These are not covered in this paper. For a thorough introduction to these issues reference can

be made to relevant chapters in the offshore geotechnical engineering books of Dean (2010) and Randolph and Gourvenec (2010), as well as to state-of-the-art review papers of Cathie *et al.* (2005), White and Cathie (2010) and Randolph *et al.* (2011).

Table 1: Notable pipelines built or currently under design offshore Western Australia

| *Name*[*] | *Operator* | *Gas/Oil* | *Length (km)* | *Diameter (mm)* | *Date* |
|---|---|---|---|---|---|
| North Rankin | North West Shelf Joint Venture | Gas | 104.4 | 1016 | 1983 |
| South Pepper Trunkline | Apache | Oil | 23.2 | 219 | 1987 |
| Chervil to Airlie Island | Apache | Oil | 6.33 | 210 | 1989 |
| Goodwyn Interfield | North West Shelf Joint Venture | Gas | 23.6 | 762 | 1993 |
| Griffin | BHP | Gas | 29.2 | 219 | 1993 |
| TSEP | North West Shelf Joint Venture | Gas | 135 | 1016 | 2003/04 |
| Bayu-Udan | Conoco Philips | Gas | 167 | 660 | 2004/05 |
| Pluto | Woodside | Gas | 180 | 914 | Construction |
| Gorgon | Chevron | Gas | 140 | 762 | Design |
| Wheatstone | Chevron | Gas | 145 | 1118 | Design |
| Ichthys | Inpex | Gas | 860 | 1066 | Design |
| Browse | Woodside | Gas | 400 | 500-1000 | Design |

*References include the Australian Pipeline Industry Association.

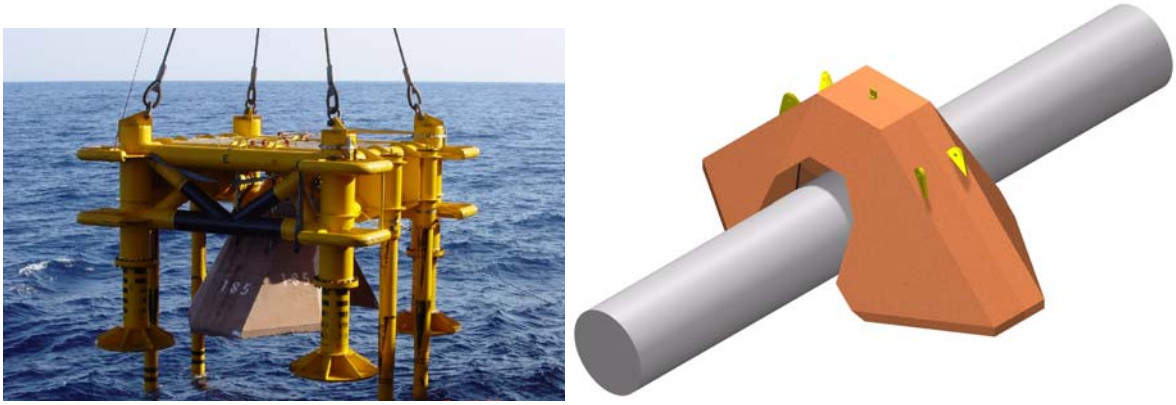

Figure 1: Example secondary anchoring solution (after Zeitoun *et al.*, 2009)

# 2 PIPELINE STABILITY DESIGN METHODS

## 2.1 INTRODUCTION

As opposed to many other regions of the world where pipelines are often placed in trenches the majority of Australian pipelines are laid directly onto the seabed. The pipes are therefore directly exposed to current and wave loading, and understanding the response to these hydrodynamic conditions forms an integral stability design criterion.

Pipelines offshore Australia are usually designed using recommended design codes, such as DNV-RP-F109 (DNV, 2007). Three approaches to the design of offshore pipelines for on-bottom stability are recommended. In order of increasing complexity these methodologies are Absolute Lateral Static Stability (ALSS), Generalized Lateral Stability (GLS) and Dynamic Lateral Stability Analysis (DLSA). The first is a simple force balance calculation and the third a comprehensive dynamic finite element analysis. As a compromise the GLS provides charts of allowable pipe weights calibrated for specific displacement criteria. They are described in order below.

## 2.2 ABSOLUTE LATERAL STATIC STABILITY (ALSS) APPROACH

ALSS represents a static equilibrium of forces acting on the pipeline. The design philosophy is that resistance of the pipe against motion should be sufficient to withstand the maximum hydrodynamic loads. If this is the case, it is assumed that the pipe will experience no lateral displacement under the design wave being considered.

The criterion for ALSS analysis is whether soil resistance on the pipe is greater than the hydrodynamic loads. Only a segment of pipe is analysed and therefore the peak hydrodynamics are conservatively assumed along the entire pipe length. For this most simplistic analysis Coulomb friction is assumed and the Morison equation used to evaluate loads, with the following formulation used to evaluate the absolute static stability:

$$\mu(W_s - F_v) > \gamma_{sc} F_h \quad \textbf{(1)}$$

where $\mu$ is the friction factor, $W_s$ is the pipeline submerged weight, $F_h$ and $F_v$ are the in-line (horizontal) and lift (vertical) hydrodynamic forces (see Figure 2 for illustration) and $\gamma_{sc}$ is the safety factor (often assumed to be 1.1 for operational pipes, see DNV, 2007; Tørnes *et al*., 2009).

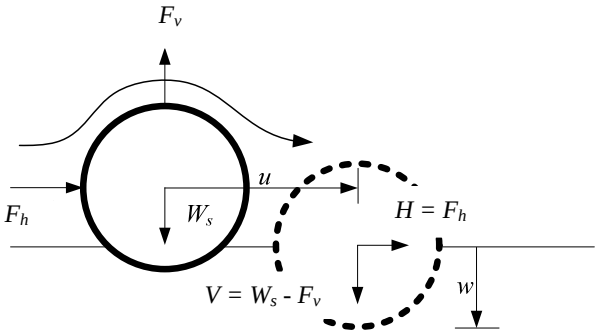


Figure 2: Definition of loads on and movement of a segment of pipe

The Morison equation is the simplest method to determine the hydrodynamic force acting on the pipe. The horizontal force and vertical lift per unit length on the member (at time $t$) can be expressed as:

$$F_h = \frac{1}{2} C_D \rho_w D (u_w + u_c)|u_w + u_c| + C_m \rho_w A \dot{u}_w \quad \textbf{(2)}$$

$$F_v = \frac{1}{2} C_L \rho_w D (u_w + u_c)|u_w + u_c| \quad \textbf{(3)}$$

where $\rho_w$ is the water density, $D$ the (hydrodynamic) cross sectional diameter of the pipe, $A$ the hydrodynamic area and $u_w$ and $u_c$ are the wave and current induced water velocities respectively. $C_D$ and $C_L$ are the horizontal and vertical (drag and lift) coefficients. For the inertia term, $\dot{u}_w$ is the acceleration of the water kinematics and $C_m$ the inertia coefficient (often assumed as 3.29 for pipe analysis). The drag term is entirely empirical and accounts for vortices created as flow passes the member, while the inertia term is due to the pressure gradient in an accelerating fluid. Unfortunately, values for $C_D$, $C_L$ and $C_m$ are empirical coefficients and their values are subjectively based on experimental data. Commonly assumed coefficients are tabulated as a function of Reynolds number (steady current only), pipe roughness, the Keulegan-Carpenter number (oscillatory flow), and the ratio of (oscillatory) wave to (steady) current. Pipeline analysis books, such as Guo *et al*. (2005), provide these factors.

In a ALSS analysis the final design weight is sensitive to the lateral resistance assumed. A single friction factor that relates lateral resistance to submerged weight, as outlined in Equation 1, is the most simplistic approach. Values of 0.6 for sands and 0.2 for clays are often assumed (Cathie *et al*., 2005; DNV, 2007). Further resistance is often assumed by considering an additional lateral passive resistance from a wedge of soil on the pipe side (an additional term is added to the left hand side of Equation 1). The frictional and passive lateral pressure components are empirically fit to laboratory data (see Wagner *et al.*, 1989; Brennodden *et al*., 1989; Verley and Sotberg, 1992; Verley and Lund, 1995; or the summary of Zeitoun *et al*., 2008).

Because the ALSS method considers the pipeline to be absolutely static it often leads to a conservative design with an overly heavy pipeline. It is also criticised for lacking a fundamental understanding of fluid-pipe-soil interaction. The use of

friction factors simplifies soil to one number and is unrelated to any understanding of the mechanics of soil behaviour. Furthermore, because it is simply based on ambient flow velocity and time invariant coefficients the Morison equation has proven incapable of accurately calculating the hydrodynamic drag and lift forces. Nevertheless, a large amount of practical experience has been accumulated using ALSS and it therefore remains the most established approach. In relatively benign conditions it may also provide an adequate calculation procedure.

### 2.3 GENERALIZED LATERAL STABILITY (GLS)

It is accepted that some movement of the pipe during large storm events should be allowed, particularly as pipelines are flexible structures. The GLS method is a set of design response figures and tables that are calibrated from numerical analyses, and which are based on an allowable displacement in a design spectrum of oscillatory wave–induced velocities running perpendicular to the pipeline. The GLS suggested from DNV (2007) are calibrated from dynamic finite element analysis by using one or ten diameters as the allowable lateral displacement criterion. The pipe soil models of Verley and Sotberg (1992) and Verley and Lund (1995) were used in this calibration. The background methodology is described by Lambrakos *et al*. (1987b) and further description of their implementation within DNV (1998, 2007) is provided in Tørnes *et al*. (2009). Though the GLS remains easy to use, it is still empirical in nature and has limited flexibility.

### 2.4 DYNAMIC LATERAL STABILITY ANALYSIS (DLSA)

DLSA requires a time domain simulation of the pipeline's dynamic response, including the time variation of hydrodynamic loads, a finite element representation of the pipe structure and an assumption of the pipe-soil boundary behaviour. The lateral displacement of a pipeline from a given combination of waves and currents for a designated sea state is calculated. A tolerable displacement limit can be set as the criterion to quantitatively evaluate the pipeline stability, providing more flexibility to tune the target reliability limits. There is also ability to conduct three-dimensional geometries and non-coherent loading, and to include different boundary conditions, such as spaced gravity anchors (e.g. Zeitoun *et al*., 2009) or a spanning pipeline (e.g. Tian and Cassidy, 2008; Tian *et al.,* 2011b).

DLSA is considered the most comprehensive method as a complete calculation is performed in the time domain. Examples of DLSA software used in industry include the American Gas Association (AGA) package and PONDUS, both of which were derived from Joint Industry Projects (Holthe *et al*., 1987; PRCI, 2002), and program SimStab developed by company JP Kenny (Tørnes *et al*., 2009; Zeitoun *et al.,* 2009). This paper outlines the development and application of new models that allow DLSA to be more easily used. This is based on the development of an in-house analysis software at The University of Western Australia (UWA) (Tian and Cassidy, 2008; Tian *et al*., 2010a, 2011b).

With increased accuracy in the hydrodynamic loading and pipe-soil models used, a more realistic result for Australian conditions is obtained. It is hoped that this will provide increased motivation for dynamic analysis tools to replace the simplified methods in industry.

## 3 ADVANCED ANALYSIS METHODS AND MODELS

Three components are required to perform a DLSA analysis: a hydrodynamic loading module, structural finite element software and a model describing the pipe-soil resistance. The in-house UWA codes have been based around the commercial Finite Element (FE) package ABAQUS, with ABAQUS structural elements and dynamic solution algorithms augmented with a pipe-soil interaction module and a hydrodynamic loading module incorporated as ABAQUS user subroutines.

### 3.1 HYDRODYNAMIC LOADING

Accurately calculating the hydrodynamic loading from storm-induced waves and currents is a critical step in evaluating the lateral stability of an offshore pipeline. As already discussed in section 2.2, the Morison equation is not an accurate model for calculating the hydrodynamic drag and lift acting on a pipe lying on the seabed. This is because it is simply based on ambient flow velocity and time invariant coefficients, and changes due to the wake sweeping back and forth over the pipe are not accounted for. The Morison equation has been shown to be especially unreliable when a current is superimposed on an irregular wave velocity (as the force coefficients are highly dependent on the current to wave ratio, $M$, and the Keulegan-Carpenter number, $K$ , see Verley *et al*., 1989; Verley and Reed, 1989; DNV, 2007). This makes it particularly problematic for application in the high current regions of the North West Shelf of Australia. More sophisticated models, such as the Wake model (Lambrakos *et al*., 1987a; Sabag *et al*., 2000) and the Fourier models (Fyfe *et al*., 1987; Bryndum *et al*., 1988; Jacobsen *et al*., 1988; Verley *et al.,* 1989; Verley and Reed, 1989), are recommended. The Wake models are similar to the

Morison equation, except that the hydrodynamic coefficients are time-dependent and the ambient velocity is modified to account for the wake effect.

Fourier models are based on the fact that a periodic variation with a certain period $T$ can be reproduced by superposition of a number of sine waves with periods of $T/i$ ($i$=1,2,3…). Fourier coefficients have been back-fitted from an extensive experimental series conducted at the Danish Hydraulics Institute and summarised, amongst others, in Sorenson *et al.* (1986), Fyfe *et al.* (1987), Bryndum *et al*. (1988), Jacobsen *et al.* (1988) and Verley and Reed (1989). A composition of nine harmonic sine waves has been shown to be sufficiently accurate to calculate the drag force component ($F_D$) of $F_h$ and $F_v$ on a pipeline:

$$F_D(t) = \frac{1}{2}\rho_w D u_w{}^2 \left[ C_0 + \sum_{i=1}^{9} C_i \cos i(\omega t - \varphi_i) \right] \quad \textbf{(4)}$$

where $\omega$ is the angular frequency ( $\omega = 2\pi / T$ ), $t$ denotes time, $u_w$ is the wave induced water velocity, and $C_i$ and $\varphi_i$ are the Fourier coefficients, which are functions of the Keulegan-Carpenter number $K$ and the current to wave ratio $M$. The Fourier models still require the inertia force $F_I$ (for $F_h$ only) to be evaluated using the same expression as the traditional Morison formulation but with a fixed inertia coefficient value of 3.29.

$$F_I(t) = 3.29\rho_w A\dot{u}_w \quad \textbf{(5)}$$

where $\dot{u}_w$ is the water particle acceleration.

Another area of conservatism in traditional approaches is that hydrodynamic forces acting on the offshore pipeline are usually calculated for a pipe just touching the seabed, with no pipe movements or embedment included. However, in practice the pipe may experience considerable movements or embedment and the hydrodynamic loads reduce. This should be accounted for and, with a sophisticated pipe-soil model tracking pipe movements, it can be. Theory to adjust the pipeline hydrodynamics forces calculated with the Fourier method is provided in Youssef *et al*. (2010).

For use in the UWA in-house analysis program, the Fourier methods were implemented into ABAQUS through use of a user subroutine DLOAD (see Dassault Systèmes, 2011 for definition of DLOAD and Youssef *et al.,* 2010 for implementation details). Named UWAHYDRO, this subroutine generates a random sea state using both the directional wave spectrum $S(\omega)$ and spreading function $D(\omega,\theta)$, evaluates the wave kinematics at the pipe position and then evaluates the hydrodynamics based on Equations 4 and 5 and the Fourier coefficients of Sorenson *et al.* (1986).

### 3.2 PIPE-SOIL MODELS

One of the major technical challenges to ensuring pipeline on-bottom stability is to accurately model pipe-soil interaction. Traditional approaches to geotechnical consideration of pipe-soil behaviour have been empirically based on bearing capacity and Coulomb frictional or two component friction and passive resistance models (e.g. Brennodden *et al*., 1989; Wagner *et al*., 1989; Verley and Sotberg, 1992; Verley and Lund, 1995). These theories are adequate though often overly conservative in predicting failure. However, the important issues of predicting plastic strains and displacements pre-failure are neglected. Difficulties in implementing many of them within structural analysis programs limit their ability to predict stability under different structural and hydrodynamic conditions. Advantages of DLSS analysis, such as three-dimensional non-coherent loading, load redistribution along the pipe and including lower loads but higher resistance with embedment, can not be realised. They are also limited in application in Australian calcareous sand conditions as they do not adequately consider the effect of cyclic loading of the pipeline, such as accumulated vertical settlement, soil densification and increased bearing capacity due to cyclic loading (Palmer *et al.,* 1988; Sawicki *et al*., 1998; Vidich *et al.,* 1998; Zhang *et al.*, 2001).

The use of plasticity theory at the macroelement scale is increasingly being considered an alternative. A segment of pipe and surrounding soil is considered as one element with the load-displacement behaviour of the entire segment described within an encapsulated force-resultant model. This offers an attractive framework as the pipe-soil response is expressed in terminology consistent with structural mechanics. This allows the significant non-linear behaviour of soils to be directly incorporated into the structural finite element packages already in use by pipeline engineers. As will be shown in this paper this provides an effective and practical approach to pipe-soil interaction modelling.

Examples of force-resultant models describing pipeline behaviour include those presented in Schotman and Stork (1987), Zhang (2001), Calvetti *et al*. (2004), Di Prisco *et al*. (2004), Hodder *et al*. (2008), Cocchetti *et al*. (2009), Hodder and Cassidy (2010) and Tian *et al*. (2010a). Two force-resultant models, describing pipes under drained and undrained behaviour, are discussed further in this paper. Zhang (2001) and Zhang *et al*. (1999, 2001, 2002a,b) developed drained pipe-soil models from centrifuge tests, which were performed on calcareous sand collected from the North West Shelf of

Australia. These models are particularly useful for analyzing offshore pipelines in this region. They were calibrated using centrifuge test data of a prototype 1 m diameter and 8 m long pipeline. The original models have been updated through more extensive centrifuge tests using calcareous silty sand collected in grab samples from a different North West Shelf site of 169 m water depth (Tian *et al.,* 2010b). These tests, and new model parameters, also provided for an extension of the applicable range of the model to lateral displacements of five diameters (Tian and Cassidy, 2011a). This latter model is described here. Hodder *et al*. (2008) and Hodder and Cassidy (2010) presented an undrained pipe-soil model from laboratory floor and a centrifuge study using Kaolin clay. Both of these force-resultant models are based within a plasticity framework and, as highlighted by Cathie *et al*. (2005) and Zeitoun *et al*. (2008), are a more theoretically valid approach than the simplistic Coulomb friction and passive resistance models.

In their simplest form both models essentially have four components: a combined vertical ($V$) and horizontal ($H$) loading yield surface defining the allowable loading conditions (for sign convention see Figure 2), a hardening law that describes the expansion of this surface with embedment, an elasticity matrix defining the elastic response for increments inside the yield surface, and a flow rule describing incremental plastic displacements during an elastic-plastic event that either expands or contracts the surface. This is essentially a single surface work-hardening plasticity model, a formulation familiar to most engineers through the one-dimensional stress-strain constitutive laws for metals. The combined vertical and horizontal load-displacement behaviour of the pipe is determined in essentially the same way as with metals, with the loading applied incrementally and the numerical plasticity model able to compute the updated tangent stiffnesses for each step. The hardening concept adopted is that at any given plastic penetration of the pipe into the soil, a yield surface of a certain size is established in combined V-H loading space. This is illustrated in Figure 3. The size of the yield surface increases as the pipe is pushed further into the soil (again see Figure 3), with slight changes in shape due to the pipe geometry also accounted for. The 'backbone' curve of vertical bearing capacity against plastic vertical penetration can be determined either theoretically or empirically. As in standard plasticity theory, changes of load within the current yield surface result only in elastic deformation. A loading path that intersects (and remains on) the yield surface also gives rise to plastic deformation, with the components of incremental plastic displacement being determined from the flow rule and hardening law.

This essentially describes the simplest elastic-plastic models of Zhang *et al.* (1999, 2001, 2002a,b), Tian and Cassidy (2008, 2011a) and the model of Hodder and Cassidy (2010). Further parameters were added to the Zhang models to account for inner surface plasticity (through use of a bounding surface terminology, Zhang *et al.*, 2002a) and also additional vertical penetration through cyclic load (through use of a second inner "bubble" surface, Zhang, 2002b).

A description of the elastic-plastic models for drained and undrained behaviour is presented here, with recommended values for the model parameters detailed in Table 2.

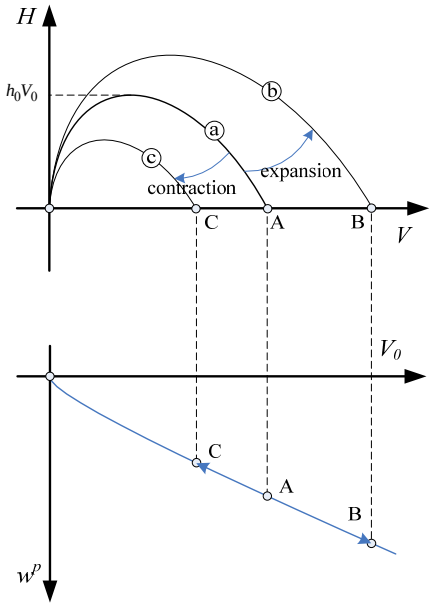


Figure 3: Theoretical assumption of hardening in plasticity models

### 3.2.1 Yield surface

The yield surface is the boundary separating the pure elastic and elastic-plastic states. The size of the yield surface denoted by $V_0$ and $h_0$ is solely related to the vertical plastic displacement $w^p$ (see Figure 2 for definition of vertical displacement $w$ and horizontal displacement $h$, and superscript $p$ denotes a plastic component). The equation for the yield surface is written directly in terms of the load ($V$, $H$) on the model (see Figure 2 for the sign convention) as:

$$F = \left(\frac{H}{h_0 V_0}\right)^2 - \beta_f{}^2 \left(\frac{V}{V_0} + \eta\right)^{2\beta_1} \left(1 - \frac{V}{V_0}\right)^{2\beta_2} = 0 \qquad \textbf{(6)}$$

where $\beta_1, \beta_2$ control the curvature of the surface (including the location of the peak horizontal force) and $\eta$ represents the normalised tensile capacity $\frac{V_t}{V_0}$, where $V_t$ is the pull out capacity. A value of $\beta_f = \frac{(\beta_1+\beta_2)^{\beta_1+\beta_2}}{\beta_1^{\beta_1}\beta_2^{\beta_2}(1+\eta)^{\beta_1+\beta_2}}$ ensures that the peak horizontal load equals $h_0 V_0$ (see illustration in Figure 3), irrespective of the values assumed for $\beta_1$ and $\beta_2$. $V_0$ is the size of the yield surface representing the bearing capacity of the pipe under a purely vertical load at the current embedment.

The parametric values defining the surface shape are provided in Table 2. These are defined through experimental constant vertical displacement tests, which are often termed "swipe" tests. In the swipe tests, a model pipeline was penetrated vertically to a prescribed vertical displacement (that also describes the surface apex under pure vertical $V_0$), before being subjected to a horizontal displacement excursion. The load path followed can be assumed to be a track across the yield surface appropriate to that penetration, assuming that the vertical elastic stiffness is much larger than the plastic stiffness (Tan, 1990). The experimental tests on calcareous sand were performed on a 1:50 scale model in a geotechnical centrifuge at 50g. A photo of the smooth model pipe of 120 mm length and 20 mm diameter is shown in Figure 4a. The undrained tests on Kaolin clay were performed on two larger pipes at 1g (diameters 20 and 70 mm and lengths 160 and 350 mm respectively, see Hodder *et al.*, 2008) and a slightly smaller 10 mm diameter and 50 mm long pipe at 50g (Figure 4b).

(a)Drained tests in beam centrifuge (b) undrained tests in drum centrifuge

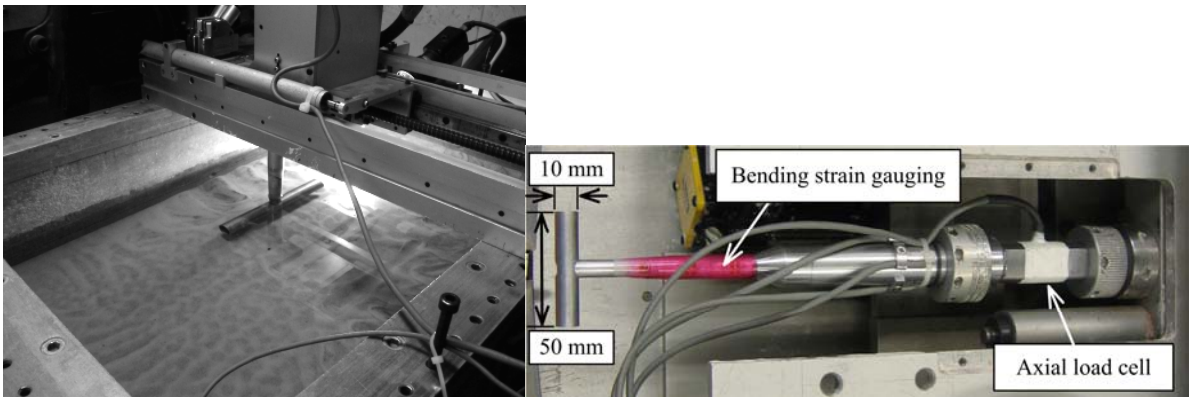


Figure 4: Model pipes used in centrifuge experiments

Example results from ten swipe tests of a pipe in calcareous silts are shown in Figure 5 (including two overloaded tests that commenced after their vertical load was reduced to 0.75 and 0.5 of the original $V_0$). Results from swipe tests in clay are shown in Figure 6. Shown in both are the fit to Equation 6.

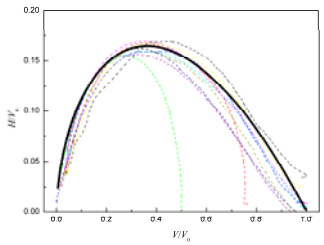


Figure 5: Example swipe test results on calcareous sands and best-fit drained yield surface

Table 2: Model parameters for macroelement elasto-plastic models and values used in numerical examples

| *Model Component* | *Constant (dim.)* | *Description* | *Value*[1] | | *Notes* |
|---|---|---|---|---|---|
| | | | *Sand* | *Clay* | |
| Geometry | D (L) | Diameter of pipe | 1 m | 1 m | See Table 1 |
| Yield Surface | $\eta$ (-) | Tensile capacity (yield surface apex as a ratio of $V_0$) | 0 | 0 to 0.75 | The undrained values are a function of embedment with values shown in Figure 7 and defined in Hodder and Cassidy (2010). |
| | $\beta_1$ (-) | Curvature factor for yield surface (low stress) | 0.53 | 0.75 | |
| | $\beta_2$ (-) | Curvature factor for yield surface (high stress) | 0.99 | 0.75 | |
| | $h_{0\ surface}$ (-) | Dimension of yield surface (horizontal: no penetration) | 0.144 | 0.147 | Represents size of the yield surface with no embedment. The undrained surface expands to 0.8 at a penetration of 3.5 diameters. Expansion of surface in drained case represented by hyperbolic function, see Hodder and Cassidy (2010). |
| | $\kappa$ (-) | Increase of yield surface size with normalised depth | 0.047 | - | |
| Hardening | $k_{vp}$ (F/L$^2$) | Hardening stiffness | 400 kPa | - | Hardening law parameters provided are best fit of experimental tests. |
| | $N_c$ | Bearing capacity factor | - | < ~10.5 | See Hodder and Cassidy(2010) for discussion and values. |
| Elasticity | $k_{he}$ (F/L$^2$) | Elastic stiffness (horizontal) | 8333 kPa | - | Drained values derived from centrifuge experiments. The vertical elastic stiffness, $k_{ve} = K_v s_{u0}$, is assumed to be proportional to the undrained shear strength. The elastic stiffness is assumed $k_{he} = 0.925 k_{ve}$, based on the solutions of Gazetas *et al*. (1985) and Gazetas and Tassoulas (1987) for a surface strip footing. |
| | $k_{ve}$ (F/L$^2$) | Elastic stiffness (vertical) | 8333 kPa | | |
| | $K_v$ | | - | 200 | |
| Flow Rule | $\alpha$ (-) | Association factor (horizontal) | 3.5 | 1.0 | Non association is more exaggerated in the drained case, with only slight adjustments in shape required in the undrained model. |
| | $\beta_3$ (-) | Curvature factor for plastic potential (low stress) | 0.025 | 0.65 | |
| | $\beta_4$ (-) | Curvature factor for plastic potential (high stress) | 0.6 | 0.65 | |

1. Parameter values as reported in Tian *et al*. (2010b), Hodder and Cassidy (2010) and Tian and Cassidy (2011a).

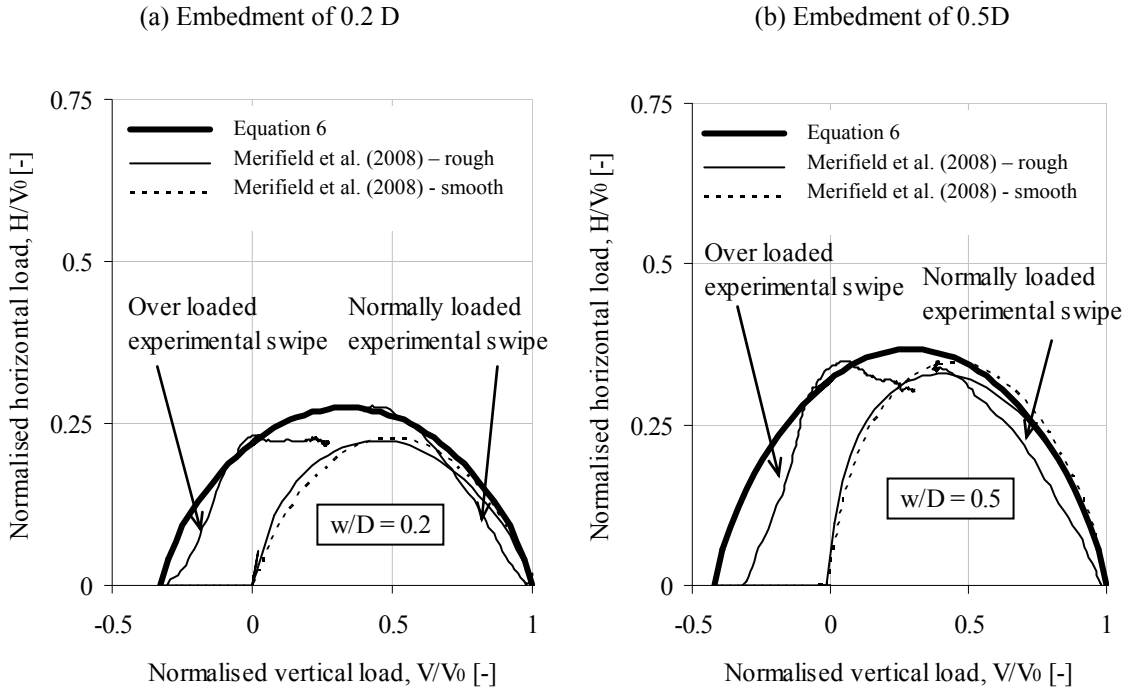


Figure 6: Swipe test results on Kaolin clay with best-fit undrained yield surface and solution of Merifield *et al.* (2008) for embedments of (a) 0.2 and (b) 0.5 diameters

One of the major differences in the parametric values reported in Table 2 is the tensile capacity assumed. For the centrifuge tests carried out under drained condition using silty sand (Tian *et al.,* 2010b), the tensile capacity is assumed to be negligible ( $\eta = 0$ ). In the case of the pipe embedded in Kaolin clay, where a tensile or suction capacity could be reasonable assumed the value of $\eta$ was fit to the experiments at a value greater than zero (with values derived from the experiments shown in Figure 7).

Other methods for deriving the shape of the yield surface have included finite element and upper bound analyses (see for instance White and Randolph, 2007; Bransby *et al.,* 2008; Merifield *et al.,* 2008 shown in Fig.6). As discussed in Hodder and Cassidy (2010), the experimental data recorded 10-35% higher horizontal capacities. This is most likely due to the additional horizontal capacity provided by the heave of soil caused by the initial penetration process and lateral motion of the swipe, which was not included in the finite element and upper bound analyses.

### 3.2.2 Hardening law

The hardening of the yield surfaces is directly correlated with the vertical plastic displacement increment $\Delta w^p$ as a change in surface size $\Delta V_0$ , as illustrated in Figure 3. An empirical relationship is used in the drained model, although a link between CPT data and bearing capacity of the pipe was discussed in Tian *et al.* (2010b). For calcareous sands the following equations fit the geotechnical centrifuge results well:

$$\Delta V_0 = \frac{k_{ve} k_{vp}}{k_{ve} - k_{vp}} \Delta w^p \qquad \textbf{(7)}$$

where $k_{ve}$ and $k_{vp}$ define the vertical elastic and plastic stiffness respectively. A hyperbolic relationship has also been suggested (Tian *et al.,* 2010b). The increase in horizontal size of the yield surface is also accounted for with $h_0$ increasing with plastic vertical penetration:

$$h_0 = h_{0surface} + \kappa \frac{w^p}{D} \qquad \textbf{(8)}$$

where $\kappa$ is the rate of growth and $h_{0\ \mathrm{surface}}$ is the $h_0$ value assumed for a surface "footing" (or in this case a pipe with zero penetration).

Bearing capacity theory for pipe penetrating clays is easier to define, with the usual definition:

$$V_0 = N_c s_{u0} D \qquad \textbf{(9)}$$

where $N_c$ is a bearing capacity factor and $s_{u0}$ the undrained shear strength of the soil at the pipe invert, used as the hardening law in the undrained model. Bearing capacity factors applicable to the penetration of cylinders into undrained soil have been presented by, amongst others, Murff *et al*. (1989), Aubeny *et al.* (2005), Barbosa-Cruz and Randolph (2005) and Merifield *et al*. (2008). As the pipe can penetrate further in soft clays (relevant to deep water applications), a more significant change in surface shape occurs. Hodder and Cassidy (2010) use a hyperbolic factor $\phi_h$ to provide a transition between the value of $h_0$ at zero embedment ($h_{0,surface}$) and that for a deeply embedded pipe ($h_{0,deep}$), which was defined to be constant at embedments greater than 3.5 diameters.

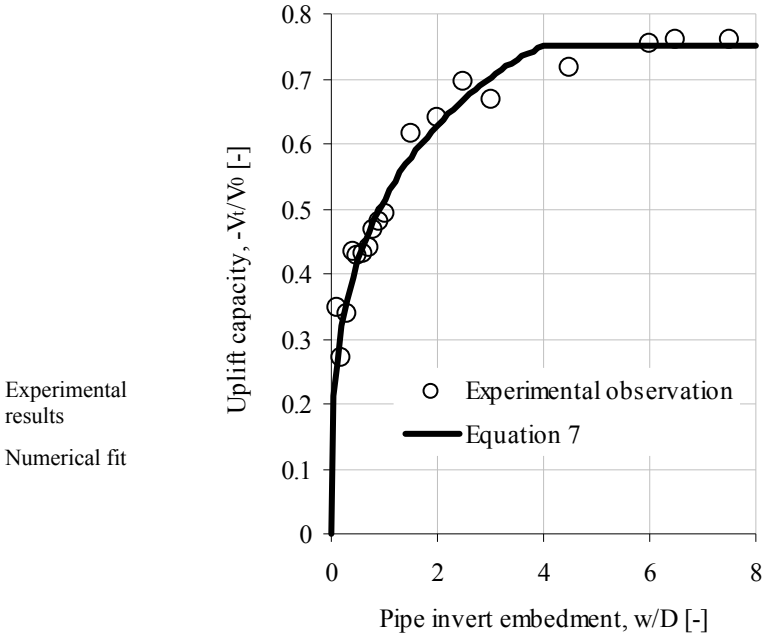


Figure 7: Variation in uplift capacity derived from centrifuge experiments of a pipe in clay

### 3.2.3 Elasticity

Elasticity describes the constitutive behaviour for increments inside the yield surface. The vertical and horizontal behaviours are regarded as an uncoupled linear relationship with the corresponding elastic displacements:

$$\begin{Bmatrix} \Delta V \\ \Delta H \end{Bmatrix} = \begin{bmatrix} k_{ve} & 0 \\ 0 & k_{he} \end{bmatrix} \begin{Bmatrix} \Delta w^e \\ \Delta u^e \end{Bmatrix} \quad \textbf{(10)}$$

where $k_{ve}$ the vertical elastic stiffness and $k_{he}$ the horizontal elastic stiffness, $\Delta$ represents an increment and the superscript *e* denotes an elastic component. Estimations of these parameters are provided in Table 2.

### 3.2.4 Flow rule

During an elastic-plastic step the relative magnitudes of the horizontal and vertical plastic displacements requires definition. Experiments involving the measurement of incremental plastic displacements at yield have been used to define suitable flow rules. These experiments have included tests that penetrate the pipe at a fixed ratio of horizontal to vertical displacement and those that follow the vertical uplift with increasing horizontal load path appropriate for wave loading. Back-calculation of the plastic displacements from these experimental tests has shown that the assumption of associated flow is not appropriate for both the drained calcareous sand and undrained clay cases. Therefore, an alternative plastic potential has been defined with a vector normal to it describing the plastic flow direction. For simplicity a non-associated plastic potential with a similar mathematic expression as the yield surface is used and is written as

$$g = \left( \frac{H}{\alpha h_0 V_0} \right)^2 - \beta_g{}^2 \left( \frac{V}{V_0} + \eta \right)^{2\beta_3} \left( 1 - \frac{V}{V_0} \right)^{2\beta_4} = 0 \quad \textbf{(11)}$$

where $\alpha$, $\beta_3$ and $\beta_4$ are the parameters controlling the plastic potential shape, with $\beta_g = \dfrac{(\beta_3+\beta_4)^{\beta_3+\beta_4}}{\beta_3^{\beta_3}\beta_4^{\beta_4}(1+\eta)^{\beta_3+\beta_4}}$ again eliminating the influence of $\beta_3$ and $\beta_4$ on the surface size (which is now defined by $\alpha h_0 V_0$). In the undrained model the apex of the surface $V_0$ is replaced by a dummy parameter $V_0'$ that defines the intersection

of the plastic potential surface that passes through the current load point with the vertical load axis (see Hodder and Cassidy, 2010 for details). By adjusting the parameters of $\alpha$, $\beta_3$ and $\beta_4$, the above equation can vary from associated ($\alpha = 1$, $\beta_3 = \beta_1$ and $\beta_4 = \beta_2$) to significant non-associated flow rule. The appropriate shape of this plastic potential has been based purely on the best fit parameters to the experimental data (see Tian *et al*., 2010b and Hodder and Cassidy, 2010 for more details).

### 3.2.5 Calculation of equivalent friction factor from plasticity models

These models of Zhang (2001), Tian *et al*. (2010b), Tian and Cassidy (2011a) and Hodder and Cassidy (2010) are based on the "critical state" concept, and therefore there exists a "parallel point" on the yield surface where sliding is predicted without the surface changing size. Theoretically this point is when the flow rule predicts zero vertical plastic penetration (the ultimate horizontal resistance $H_{ult}$ at a vertical load when $\frac{\partial g}{\partial V} = 0$). By referring back to the terminology of a Coulomb friction model (see Equation 1), the ultimate friction factor is achieved by normalizing the ultimate lateral resistance with the vertical force (defined here as $\mu^* = \frac{H_{ult}}{V \mid \left(\frac{\partial g}{\partial V} = 0\right)}$). The theory to describe how this is calculated will not be covered here. However, the factors derived for the plasticity models of Zhang (2001) and Hodder and Cassidy (2010) with embedment are shown in Figure 8. As expected these increase with depth. The values of DNV (2007), as described in section 2.2, can be seen to be conservative when the pipeline embedment is not accounted for.

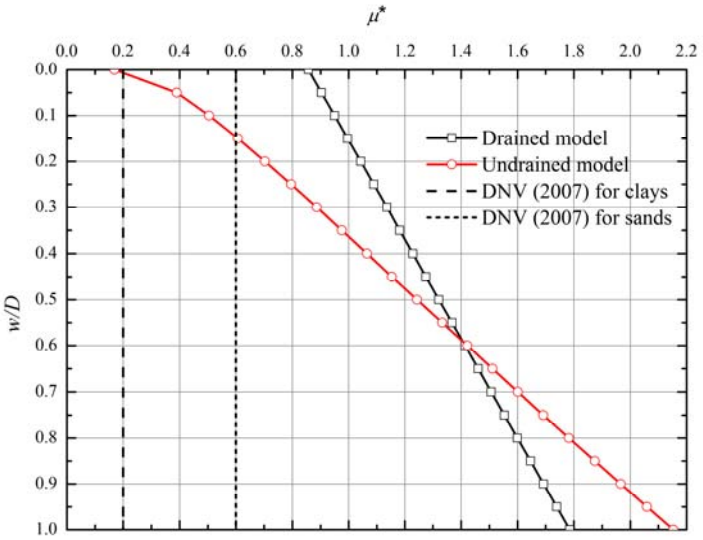


Figure 8: Equivalent friction factors derived from plasticity models

## 3.3 STRUCTURAL MODELLING

Standard ABAQUS elements are used to represent the pipeline. We generally use ABAQUS B31H beam elements, though B31, B32 and B33 elements can suffice (see Dassault Systèmes, 2011 for element details). B31H is a 2-noded beam element with linear interpolation and a hybrid formulation. The hybrid beam is more numerically robust to compute the axial and shear forces when the beam undergoes large rotations.

The numerical module describing the constitutive behaviour of pipe-soil model and the hydrodynamic module of UWAHYDRO interact with ABAQUS in the following way:

**Set-up:**

i. The sea state and hydrodynamic loading is calculated and stored in a DLOAD database (i.e. the hydrodynamic loads at each node are calculated for the storm assuming the pipe invert is just touching the soil surface, as described in Section 3.1).
ii. The pipe-soil models are initialised for the pipe laying process (using Equation 7 or 9). This is conducted as soil underneath the pipeline is subjected to larger vertical loads than the pipeline submerged self-weight

during pipe laying, as a long length of pipe hangs suspended between the pipe-laying vessel and the seabed (Cathie *et al*., 2005; Tian and Cassidy, 2008b; Tian and Cassidy, 2010). To account for this numerically, the models are expanded to the higher pipe laid $V_0$ before being reduced (inside the combined yield surface) to the self-weight. At the start of the loading analysis the pipe is in equilibrium with the submerged self-weight applied, but already embedded to the vertical displacement corresponding to the higher as laid weight.

**Time-domain storm analysis:**

iii. At each new solution increment (or equilibrium iteration), say at time $t_n$, the pipe-soil model at each element is provided with the incremental displacements of the corresponding node it is attached to (initially zero).
iv. This incremental displacement is used by each pipe-soil model to determine the corresponding internal forces, state variables and the tangent stiffness matrix at the end of the increment. These are in turn delivered back to the main program ABAQUS.
v. ABAQUS assembles the global stiffness and calls DLOAD to obtain the incremental load (at this stage the hydrodynamic loads stored in the DLOAD database can be adjusted for pipeline movements and embedments, see Youssef *et al*., 2010).
vi. The overall solution of the non-linear equations is solved and the increment is filtered and passed to the macroelement pipe-soil models for the next iteration.

The steps iii to vi are iterated in a Newton-Raphson scheme until convergence is reached (see Tian and Cassidy 2008, 2010a for details). A full comparison on the most efficient and accurate solutions algorithms for macroelement modelling is provided in Tian and Cassidy (2010a). The major challenge is the large number of elements (over a hundred) often needed in a long three-dimensional pipeline analysis.

# 4 EXAMPLE ANALYSIS

In this example we aim to show the benefit of using a DLSS approach with a sophisticated macroelement plasticity model. A pipeline of 1250 m in length resting on calcareous sand and in water depth of 50 m is analysed. During a one hour storm of intensity described by a JONSWAP spectrum with significant wave height of $H_s = 10$ m and zero mean crossing period $T_z = 10$ s (Table 3) the hydrodynamic loads shown in Figure 9 were calculated for the middle segment of pipe. It is noted that because of spatial dispersion the loads along the pipe are not the same at each point in time. This is highlighted in Figure 10, which shows the hydrodynamic loads along the full 1250 m of pipe at 1200 s into the storm. All of these loads are calculated using the Fourier methods of Equations 4 and 5, the Fourier coefficients of Sorenson *et al*. (1986), and as implemented in the UWAHYDRO program. In calculating these loads the pipe was assumed to be resting with its invert on the soil surface.

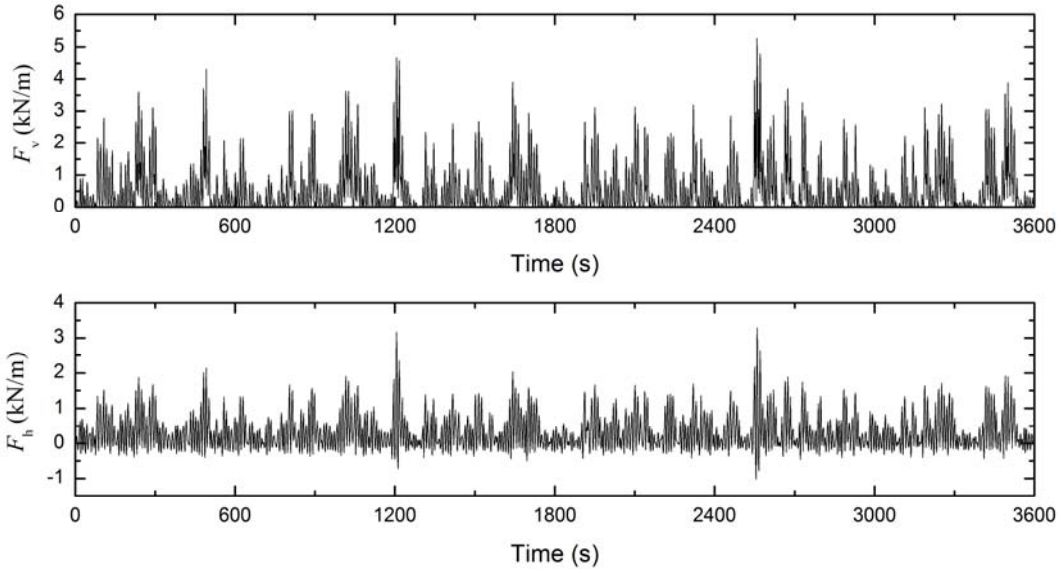


Figure 9: Hydrodynamic loads acting on the middle 5 m of pipe during a one hour storm

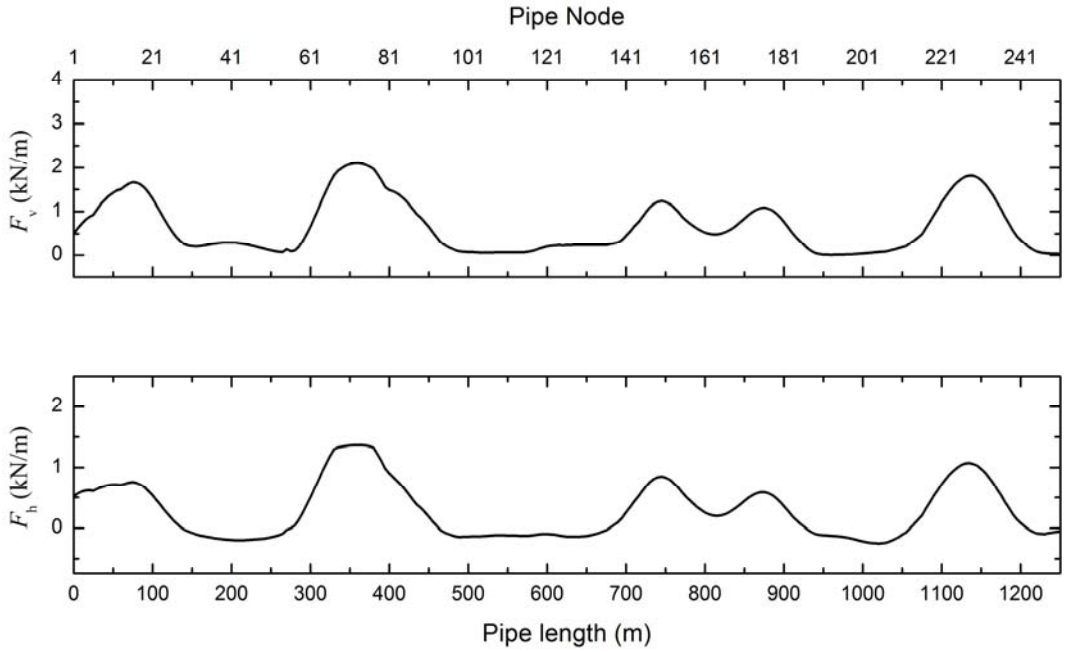


Figure 10: Hydrodynamic loads acting along the pipe at t = 1200s during the same storm

Table 3: Hydrodynamic and structural values used in numerical analysis

| *Type* | *Parameter* | *Value* |
|---|---|---|
| Storm conditions | Water depth | 50 m |
| | Wave spectrum | JONSWAP |
| | $H_s$ | 12 m |
| | $T_z$ | 10 s |
| | Current | 1 m/s |
| Pipe geometry | Length | 1250 m |
| | Diameter | 1 m |
| | Pipe self-weight ($W_s$) | 5.26 kN/m |
| | Vertical load amplification during lay (initial $V_0$) | 2 (10.52 kN/m) |

A simple design using the ALSS method of Equation 1 is first described. Because the ALSS is for a segment of pipe, only the middle 5 m was analysed. For ease of interpretation the loads acting on this segment have been replotted with the horizontal resultant forces ($F_y$) against the vertical resultant force ($W_s$-$F_z$) in Figure 11. A total of 3600 dots are included, each representing an interval of 1 s. Also shown is the frictional design curve for a friction factor of $\mu = 0.6$ and a safety factor of $\gamma_{sc} = 1.1$. According to Equation 1, all load points to the right hand side of the line are safe and those on the left hand side represent failing scenarios for the ALSS method. This figure has been developed for a pipe weight of 5.26 kN/m (Table 3). A safe design could be developed by increasing the pipe weight, say to 10.83 kN/m, allowing all of the load points to move to the safe right hand side of the curve. This is shown in Figure 12. The increase of 5.57 kN/m amounts to an extra 6 cm of high density (3050 kg/m$^3$) concrete coating. However, this increase in weight would represent a sizable economic cost, and possibly even prove impossible to lay. Secondary stabilization methods could also be considered, though ALSS does not provide a means to analyse their contribution.

The same sea state has been analysed as DLSS using the in-house UWA dynamic analysis software. The drained elasto-plastic model with the parameters outlined in Table 2 has been assumed. The structural properties assumed are provided in Table 3. A total of 250 B31H elements have been used and 251 pipe-soil models attached at the nodes, as shown in Figure 13.

Before the hydrodynamic loads were applied vertical loads imitating the pipe laying effect were applied to the model, before being reduced to the pipe self-weight (step ii of section 3.3). In this example this load concentration factor is taken as 2. That is, the pipe was loaded to twice the submerged self-weight ($2W_s$) and unloaded to self-weight ($W_s$) before hydrodynamic loading generated from UWAHYDRO was applied

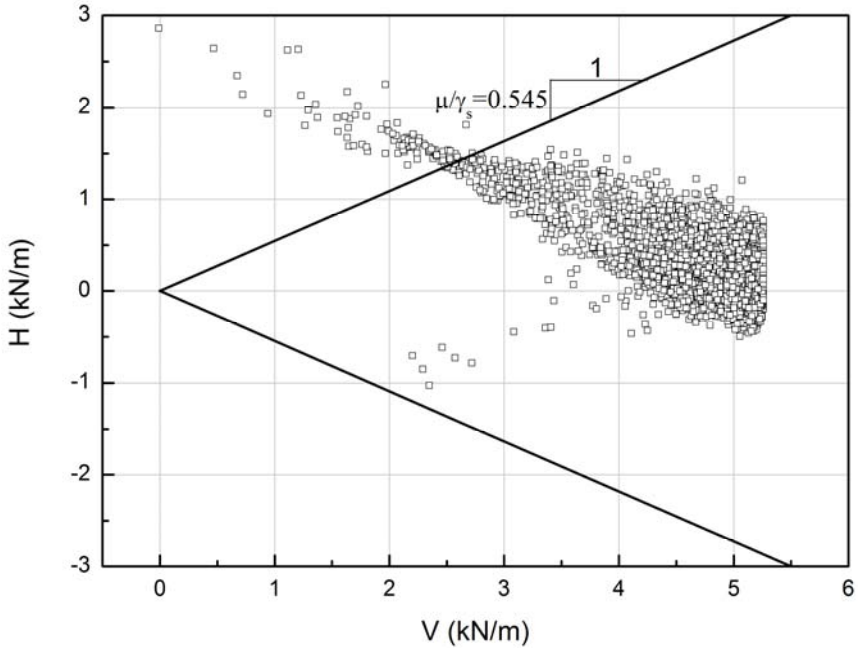


Figure 11: Design chart for middle segment of pipe

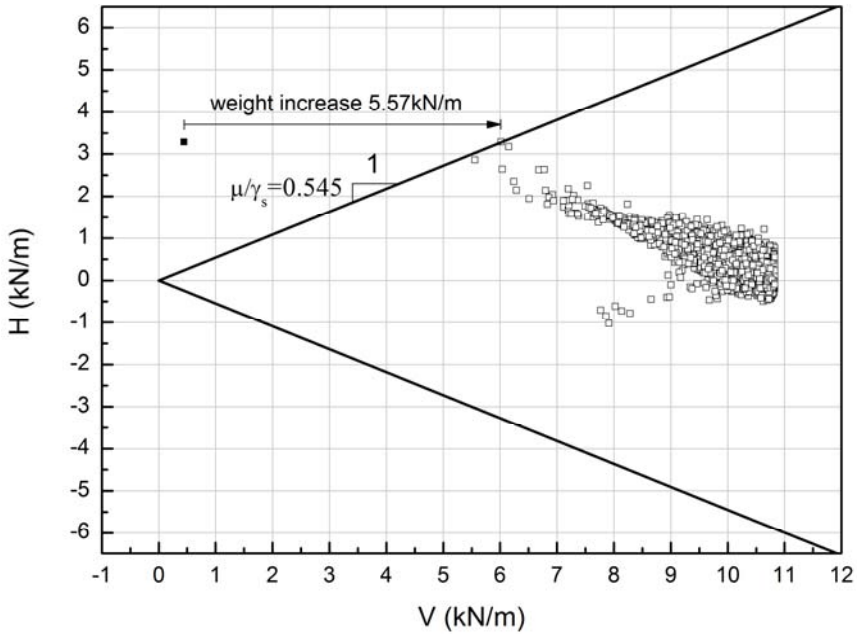


Figure 12: Safe ALSS design by increasing the self-weight to 10.83 kN/m

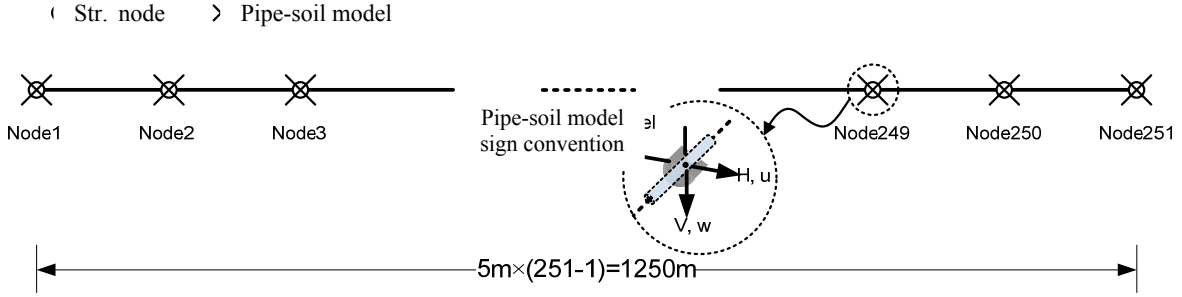


Figure 13: Computational model illustration

The final pipeline configuration after the 1 hour storm is illustrated in Figure 14. The maximum horizontal displacement was calculated as 6.89 m. This was for loads calculated assuming the pipe's invert rests on the soil surface, as shown in Figures 9 and 10. The significant advantage of including hydrodynamic reduction due to pipeline movement and embedment is shown in Figure 14, with the maximum lateral displacement in that case being 3.81 m. By calculating the absolute displacements a serviceability state can be imposed by the designer (or operator!). In this scenario, with only a lateral displacement of 3.81 or 6.89 m (or diameters for this 1 m diameter pipe), the pipe could be deemed stable.

Reasons why the DLSS has provided a less conservative design include the following.

The spatial variability of the hydrodynamic loads is used (i.e. the peak loads are not predicted to be acting on each segment of pipe at the one time, see Figure 10).

Loads can be redistributed along the pipe to sections of higher constraint. Often a segment of pipe starts to slide (with loading conditions on the parallel point of the plasticity model). In a two-dimensional analysis of a pipe segment, no more load could be added to this pipe. However, in a three-dimensional model any additional loads can be redistributed to the neighbouring sections of pipe where the pipe-soil model may still predict restraint.

Embedment of the pipe model due to the laying process and also through additional penetration due to the cyclic horizontal loads provides for additional restraint within the pipe-soil models (though not shown here this effect is enhanced by use of the cyclically embedding "bubble" model of Zhang *et al.*, 2002b and Tian and Cassidy 2011b).

By calculating the pipe movement and embedment at each segment of pipe, appropriate hydrodynamic reductions can be applied. This reduced the maximum lateral displacement from 6.89 to 3.81 m in this example.

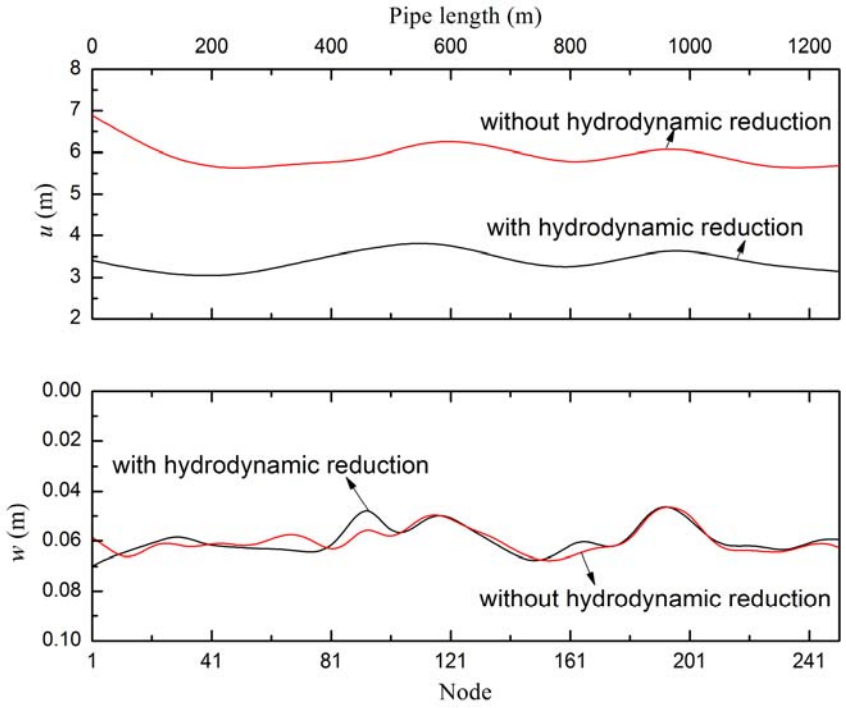


Figure 14: Final pipeline configurations

## 5 CONCLUSIONS

This paper has provided a review of design approaches taken for assessing the stability of Australia's untrenched pipelines when subjected to the hydrodynamic loading from waves and currents. The three main approaches used by industry were discussed and their advantages and disadvantages assessed. In a design example one hour of a large storm was analysed along a 1.25 km long pipe in 50 m water depth. The simpler force balance method required a significant increase in primary pipe weight to be deemed stable, whilst the major benefit of conducting the more comprehensive dynamic time domain simulation was emphasised. The ability of a macroelement plasticity model that describes pipe-soil behaviour for Australian calcareous sands and silts to be incorporated within the finite element program ABAQUS was demonstrated.

The two calculation cases shown in this paper were carried out on a single-thread desktop computer with 2.50 GHz CPU and 2.49 GByte of memory. The cases took 7 hours and 35 minutes and 6 hours and 40 minutes to run. This is the typical running time for these types of dynamic analyses, though the speed can be improved remarkably by customizing some control parameters of the program. For instance, the program has the functionality for advanced users to select computational algorithms, which will speed up the calculation noticeably. This is discussed in Tian and Cassidy (2010a).

Benefits of the dynamic time domain analysis include the capacity to analyse spatially varying hydrodynamic loads, redistribute them along the pipe if soil failure in one section is predicted, incorporate hydrodynamic reductions due to pipe movements and for the designer to set a displacement limit criteria.

## 6 ACKNOWLEDGEMENTS

The UWAHYDRO program was written with Mr Bassem Youssef as part of his PhD research. The authors gratefully acknowledge the financial contributions of the CSIRO Flagship Collaboration Fund and the Australia-China Natural Gas Technology Partnership Fund to this research. The first author is the recipient of an Australian Research Council Future Fellowship and holds the Chair of Offshore Foundations from The Lloyd's Register Educational Trust, an independent charity working to achieve advances in transportation, science, engineering and technology education, training and research worldwide for the benefit of all. This research also forms part of the recently established Australian Research Council Centre of Excellence for Geotechnical Science and Engineering.

## 7 REFERENCES

Aubeny, C.P., Shi, H. and Murff, J.D. (2005). "Collapse loads for a cylinder embedded in trench in cohesive soil". *Int. J. Geomechanics, ASCE* 5(4): 320–325.

Barbosa-Cruz, E.R. and Randolph, M.F. (2005). "Bearing capacity and large penetration of a cylindrical object at shallow embedment". *Proc. Int. Symposium on Frontiers in Offshore Geotechnics*, Perth, Australia. 615-621.

Bransby, M.F., Amman, S. and Zajac, P. (2008). "Numerical analysis of the capacity of 'on-bottom' offshore pipelines". *Proc. 2nd BGA Int. Conf. on Foundations*, Dundee, Scotland.

Brennodden, H., Lieng, J.T. and Sotberg, T. (1989). "An energy-based pipe-soil interaction model". *Proc. of the 21st Offshore Technology Conference*, Houston, USA.

Brown, N.B., Fogliani, A.G. and Thurstan, B. (2002). "Pipeline lateral stabilisation using strategic anchors". *Proc. of the Society of Petroleum Engineers (SPE) Asia Pacific Oil and Gas Conference*, Melbourne, Australia.

Bryndum, M.B., Jacobsen, V. and Tsahalis, D.T. (1988). "Hydrodynamic forces on pipelines: model tests". *Proc. 7th Offshore Mech. and Arctic Eng. Conf.* ASME.

Calvetti, F., Di Prisco, C. and Nova, R. (2004). "Experimental and numerical analysis of soil-pipe interaction." *Journal of Geotechnical and Geoenvironmental Engineering ASCE*, 130(12): 1292-1299.

Cathie, D. N., Jaeck, C., Ballard, J.-C. and Wintgens, J.-F. (2005). "Pipeline seotechnics – State-of-the-art". *Proc. of the Int. Symp. on the Frontiers in Offshore Geotechnics: ISFOG 2005*, Perth, Australia, 95-114.

Cocchetti, G., di Prisco, C., Galli, A. and Nova, R. (2009). "Soil-pipeline interaction along unstable slopes: a coupled three-dimensional approach. Part 1: Theoretical formulation. *Canadian Geotechnical Journal*, 46:1289-1304.

Dassault Systèmes (2011). "Abaqus analysis user's manual", Simula Corp. Providence, RI, USA.

Dean, E.T.R. (2010). "Offshore geotechnical engineering". Thomas Telford.

Di Prisco, C., Nova, R. and Corengia, A. (2004). "A model for landslide-pipe interaction analysis". *Soils and Foundations* 44(3): 1-12

DNV (1998). "On-bottom stability design of submarine pipelines". Recommended practice DNV RP-E305". Det Norsk Veritas.

DNV (2007). "On-bottom stability design of submarine pipelines". Recommended practice DNV RP-F109. Det Norsk Veritas.

Fyfe, A.J., Myrhaug, D. and Reed, K. (1987). "Hydrodynamic forces on seabed pipelines: large scale laboratory experiments". *Proc. of the 19th Offshore Technology Conference*, Houston, USA.

Gazetas, G., Dobry, R. and Tassoulas, J.L. (1985). "Vertical response of arbitrarily shaped embedded foundations". *Journal of Geotechnical Engineering, ASCE.* 111(6): 750-771.

Gazetas, G. and Tassoulas, J.L. (1987). "Horizontal stiffness of arbitrarily shaped embedded foundations". *J. Geotech. Eng.* 113(5): 440-457.

Guo, B., Song, S., Chacko, J. and Ghalambor, A. (2005). "Offshore pipelines". Elsevier.

Hodder, M.S. and Cassidy, M.J. (2010). "A plasticity model for predicting the vertical and lateral behaviour of pipelines in clay soils". *Géotechnique*, 60(4): 247-263.

Hodder, M.S., Cassidy M.J., Barrett, D. (2008). "Undrained response of shallow pipelines subjected to combined loading". *Foundations: Proc. of the 2nd British Geotechnical Association Int. Conf. on Foundations*, ICOF2008, *IHS BRE Press*, Dundee, UK, 897-908.

Holthe, K., Sotberg, T. and Chao, J.C. (1987). "An efficient computer program for predicting submarine pipeline response to waves and current. *Proceedings of the 19th Offshore Technology Conference*, Houston, USA.

Jacobsen, V., Bryndum, M.B. and Tsahalis, D.T. (1988). "Prediction of irregular wave forces on submarine pipelines". *Proc. 7th Offshore Mech. and Arctic Eng. Conf.* ASME.

Lambrakos, K.F., Chao, J.C., Beckmann, H. and Brannon, H.R. (1987a). "Wake model of hydrodynamic-forces on pipelines". *Ocean Engineering* 14(2): 117-136.

Lambrakos, K.F., Remseth, S., Sotberg, T., Verley, R.L.P. (1987b). "Generalised response of marine pipelines", *Proc. of the Offshore Technology Conference*, Houston, USA, OTC5507.

Merifield, R.S., White, D.J., Randolph, M.F. (2008). "Analysis of the undrained breakout resistance of partially embedded pipelines". *Géotechnique*, 58(6): 461-470.

Murff, J.D., Wagner, D.A., Randolph, M.F. (1989). "Pipe penetration in cohesive soil". *Géotechnique*, 39(2):213-229.

Palmer, A.C., Steenfelt, J.S., Steensen-Bach, J.O., Jacobsen, V. (1988). "Lateral resistance of marine pipelines on sand." *Proc. of the Offshore Technology Conference,* Houston, USA, OTC5853.

PRCI (2002). "Submarine pipeline on-bottom stability". PRCI. Project Number PR-178-01132

Randolph, M.F., Gaudin, C., Gourvenec, S., White, D.J., Boylan, N., Cassidy, M.J. (2011). "Recent advances in offshore geotechnics for deepwater oil and gas developments". *Ocean Engineering*, 38(7): 818-834.

Randolph, M.F. and Gourvenec, S. (2010). "Offshore geotechnical engineering". Taylor and Francis.

Sabag, S.R., Edge, B.L. and Soedigdo, I. (2000). "Wake Ii model for hydrodynamic forces on marine pipelines including waves and currents". *Ocean Engineering*, 27(12): 1295-1319.

Sawicki, A., Swidzinski, W., and Zadroga, B. (1998). "Settlement of shallow foundations due to cyclic vertical force." *Soils Found.*, 38(1): 35–43.

Schotman, G.J.M. and Stork, F.G. (1987). "Pipe-soil interaction: A model for laterally loaded pipelines in clay. *Proc. of the Offshore Technology Conference*, Houston, USA.

Sorenson, T., Bryndum, M. and Jacobsen, V. (1986). "Hydrodynamic forces on pipelines - model tests. Danish Hydraulic Institute (DHI). Contract PR-170-185. Pipeline Research Council International Catalog No. L51522e

Tan, F.S.C. (1990). "Centrifuge and theoretical modeling of conical footings on sand". PhD Thesis, Cambridge University.

Tian, Y. and Cassidy, M.J. (2008). "Modelling of pipe-soil interaction and its application in numerical simulation". *Int. J. Geom. ASCE* 8(4): 213-229.

Tian, Y. and Cassidy, M.J. (2010a). "The challenge of numerically implementing numerous force-resultant models in the stability analysis of long on-bottom pipelines". *Computers and Geotechnics*, 37(1-2): 216-312.

Tian, Y. and Cassidy, M.J. (2011a). "A pipe-soil interaction model incorporating large lateral displacements in calcareous sand". *Journal of Geotechnical and Geoenvironmental Engineering*, ASCE, 137(3): 279-287.

Tian, Y., Cassidy, M.J. and Gaudin, C. (2010b). "Advancing pipe-soil interaction models through geotechnical centrifuge testing in calcareous sand". *Applied Ocean Research*, 32(3): 294-297.

Tian, Y., Cassidy, M.J., Youssef, B.S. (2011b). "Consideration for on-bottom stability of unburied pipelines using a dynamic fluid-structure-soil simulation finite element program". *International Journal of Offshore and Polar Engineering.* 21(3): 1-8.

Tørnes, K., Zeitoun, H., Cumming, G. and Willcocks, J. (2009). "A stability design rationale - a review of present desgin approaches". *Proceedings of the ASME 2009 28th International Conference on Ocean, Offshore and Arctic Engineering*, Honolulu, Hawaii, USA.

Verley, R.L.P., Lambrakos, K.F. and Reed, K. (1989). "Hydrodynamic-forces on seabed pipelines". *Journal of Waterway Port Coastal and Ocean Engineering-ASCE*, 115(2): 190-204.

Verley, R.L.P. and Lund, K.M. (1995). "A soil resistance model for pipelines placed on clay soils". *Proceedings of the 14th International Conference on Offshore Mechanics and Arctic Engineering*, Copenhagen, Denmark.

Verley, R.L.P. and Reed, K. (1989). "Use of laboratory force data in pipeline response simulations". *Proceedings of the 8th International Conference on Offshore Mechanics and Arctic Engineering*. The Hague, Netherlands

Verley, R.L.P. and Sotberg, T. (1992). "Soil resistance model for pipelines placed on sandy soils". *Proceedings of the 11th International Conference on Offshore Mechanics and Arctic Engineering*. Alberta, Canada

Vidich, S.D., Kulhawy, F.H., and Trautmann, C.H. (1998). "Laboratory modeling of inclined-loaded shafts in sand." *Geotech. Test. J.*, 21(3): 203–212.

Wagner, D. A., Murff, J. D., Brennodden, H. and Sveggen, O. (1989). "Pipe-soil interaction-model". *Journal of Waterway Port Coastal and Ocean Engineering, ASCE*, 115(2): 205-220.

White, D.J. and Cathie, D.N. (2010). "Geotechnics for subsea pipelines". *Proc. of the 2nd Int. Symp. on the Frontiers in Offshore Geotechnics: ISFOG 2005*, Perth, Australia, 87-122.

Youssef, B.S., Cassidy, M.J. and Tian, Y. (2010). "Balanced three-dimensional modelling of the fluid-structure-soil interaction of an untrenched pipeline. *Proc. of the 20th International Offshore (Ocean) and Polar Engineering Conference*, Beijing, China.

Zhang, J. (2001). "Geotechnical stability of offshore pipelines in calcareous sand". PhD Theisis, The University of Western Australia.

Zhang, J., Randolph, M.F., Stewart, D.P. (1999). "Elasto-plastic model for pipe-soil interaction of unburied pipelines". *Proc. of the 9th Int. Symp. Offshore and Polar Engineering (ISOPE)*, 2: 185–192.

Zhang, J., Stewart, D.P., Randolph, M.F. (2001). "Centrifuge modeling of drained behavior for pipelines shallowly embedded in calcareous sand." *Int. J. Physical Modeling in Geotechnics*, 1:25–39.

Zhang, J., Stewart, D.P., Randolph, M.F. (2002a). "Modelling of shallowly embedded offshore pipelines in calcareous sand". *Journal of Geotechnical and Geoenvironmental Engineering ASCE* 128(5): 363-371.

Zhang, J., Stewart, D.P., and Randolph, M.F. (2002b). "Kinematic Hardening Model for Pipeline-Soil Interaction under Various Loading Conditions". *The International Journal of Geomechanics ASCE*, 2(4), 419-446.

Zeitoun, H., Tørnes, K., Cumming, G., Branković, M. (2008). "Pipeline stability - State of the art". *Proceedings of the 27th International Conference on Offshore Mechanics and Arctic Engineering*, Estoril, Portugal.

Zeitoun, H., Tørnes, K., Li, J., Wong, S., Brevet, R. and Willcocks, J. (2009). "Advanced dynamic stability analysis". *Proceedings of the 28th International Conference on Ocean, Offshore and Arctic Engineering*, Honolulu, Hawaii, USA.